Femtosecond Electron and Spin Dynamics in Gd(0001) Studied by Time-Resolved Photoemission and Magneto-optics

M. Lisowski, P. A. Loukakos, A. Melnikov, I. Radu, L. Ungureanu, M. Wolf, and U. Bovensiepen*

Freie Universität Berlin, Fachbereich Physik, Arnimallee 14, 14195 Berlin-Dahlem, Germany

(Received 13 April 2005; published 22 September 2005)

Femtosecond electron and spin dynamics of the Gd(0001) surface are investigated by time-resolved photoemission and second harmonic generation. Upon optical excitation the spin polarization of the surface state is reduced by half while its exchange splitting remains nearly unchanged. Electron-magnon interaction is proposed to facilitate electron-spin-flip scattering among spin-mixed surface and bulk states, which provides a mechanism for ultrafast demagnetization.

DOI: 10.1103/PhysRevLett.95.137402 PACS numbers: 78.47.+p, 73.20.−r, 75.40.Gb, 79.60.−i

A microscopic understanding of elementary excitations in ferromagnets is important from a scientific point of view as well as for applications such as ultrafast laser-assisted magnetic recording. The mechanism which is responsible for the reduction of the magnetization M with increasing temperature T has been debated for decades [1]. The Stoner model, which is appropriate for delocalized spins, proposes a decrease in the exchange interaction with T proportional to $M(T)$. For localized spins, on the other hand, fluctuations and excitations of magnetic moments lower M while the exchange interaction is not affected by T. This is referred to as spin-mixing behavior [2]. Neutron scattering experiments of $3d$ itinerant ferromagnets such as Fe, Co, and Ni provide evidence for spin waves and local magnetic moments even above the Curie temperature T_C, which suggests a localized character of spins [3]. However, a Stoner-like collapse of the exchange splitting of majority and minority subbands at T_C observed in photoemission emphasizes their itinerancy, because the quasifree valence electrons average over spatial fluctuations of the local spin density [4,5]. It has been concluded that neither of these simple models accounts for the temperature dependent properties since $3d$ spins exhibit localized and delocalized contributions in parallel [6]. Both have been included in a generalized Hubbard model [7].

In lanthanides the magnetic moment μ is dominated by the spins of $4f$ electrons. The latter are localized at the ion core, polarize the valence band and generate an itinerant contribution to μ. In Gd the exchange splitting of valence electrons Δ_{ex} is reduced with increasing temperature but remains finite above T_C while the spin polarization vanishes [2,8]. On Gd(0001) the exchange-split $5d_{z^2}$ surface state has been studied extensively [8–14]. Since at T_C its exchange splitting is finite ($\Delta_{ex} = 0.4$ eV) [11], the surface state exhibits an analogous behavior to bulk Gd. This feature, which is not described by the Stoner model, can be conceived by taking into account that the coherence length of valence electrons can be smaller than regions of spin fluctuations in the thermally activated system [2,9]. Overall, in Gd neither Stoner behavior nor spin-mixing prevails [8,10] and an understanding of magnetic quasiparticle excitations is still challenging.

One way to study these processes is to perform pump-probe experiments to reach the femtosecond time scale of elementary spin excitations. Up to now such investigations have focused on $3d$ ferromagnets using magneto-optical methods [15–19], photoemission (PE), [20,21], and theory [22]. Basically all these studies conclude that after optical excitation ultrafast demagnetization occurs within several 100 fs. Various mechanisms based on spin-orbit, electron-spin, and phonon-spin interaction have been discussed [23,24] but the responsible elementary process has not been identified to date.

In this Letter, we combine time-resolved photoemission (TRPE) and nonlinear magneto-optics on the Gd(0001) surface to investigate the transient evolution of the exchange splitting and the spin polarization under comparable conditions. While both the bulk and surface are excited by the pump laser pulse, we probe the dynamics selectively through the surface state which we consider as a model system due to its localization and large Δ_{ex}. By this approach we identify spin-flip scattering of valence electrons which leads to magnon emission or absorption including the $4f$ moments as the process responsible for a loss of spin polarization on the femtosecond time scale.

Epitaxial Gd(0001) films of ~10 nm thickness are grown on W(110) in ultrahigh vacuum (UHV) [25]. For TRPE, laser pulses at $h\nu_1 = 1.5$ eV with 55 fs duration and 4 μJ pulse energy are generated by an amplified Ti:sapphire laser system at 300 kHz. A 3 μJ portion delivers s-polarized pump pulses and 1 μJ is used to generate time-delayed 90 fs p-polarized probe pulses at $h\nu_2 = 6.0$ eV. Both beams are focused onto the Gd surface kept in UHV at $T = 100$ K. The absorbed pump fluence is typically 1 mJ/cm^2. The kinetic energy of photoelectrons is analyzed in normal emission by a time-of-flight spectrometer (TOF) [26]. In a second setup a cavity-dumped Ti:sapphire oscillator generates 1.5 eV laser pulses with 35 fs duration at 760 kHz and similar pump fluence. We detect the intensity of optical second harmonic generation

(SHG) $I^{\uparrow,\downarrow}$ for opposite directions of M [25]. $I^{\uparrow,\downarrow}$ consists of fields $E^{2\nu}_{\text{even}}$ and $E^{2\nu}_{\text{odd}}$ which behave as either even or odd with respect to the reversal of M [27]. The transient $E^{2\nu}_{\text{odd}}(t)$ determined by $I^{\uparrow}(t) - I^{\downarrow}(t)$ is proportional to pump-induced changes of the surface state's spin polarization [25] which is measured sensitively due to a resonant SHG enhancement through the surface state [28].

The time-resolved magneto-optical signal $E^{2\nu}_{\text{odd}}$ displayed in Fig. 1 represents a drop to 50% of the equilibrium spin polarization within the pulse duration. The pronounced oscillations with a period of 340 fs are driven by a coherent phonon [25]. Comparable transients are observed for lower pump fluences. The incoherent part determined by subtraction of the oscillatory component [25] is displayed for different pump fluence since in the present context the coherent part is of minor importance. The initial drop in $E^{2\nu}_{\text{odd}}$ increases linearly with pump fluence, which asks for an ultrafast mechanism that is mediated by optically excited electrons since at the employed fluence optically driven spin reversal can be ruled out [22]. Dichroic bleaching effects discussed for magneto-optics in $3d$ ferromagnets [17,18] can be disregarded here because the electron population decays within 1 ps (Fig. 2), but the drop in the magnetic transient remains from 0.1 up to 40 ps. Recovery of $E^{2\nu}_{\text{odd}}$ occurs on a 100 ps time scale and originates from lattice cooling through spin-lattice interaction [29].

To investigate the pump-induced variation of the exchange-split electronic structure, we employed TRPE. The top panel of Fig. 2 displays a spectrum around E_F at 300 fs with the PE yield measured over 5 orders of magnitude. The occupied surface state $S^{\uparrow}$ is readily visible, while the unoccupied component $S^{\downarrow}$ shows up as a shoulder 0.4 eV above E_F. To fit the spectra two Lorentzians for $S^{\uparrow,\downarrow}$, a constant bulk density of states and a distribution function $f(E, t)$ are used [30]. Convolution with a Gaussian of 45 meV width accounts for broadening from the laser pulse and the spectrometer resolution. As shown in Refs. [5,21], unoccupied states can be analyzed with photoemission by normalizing the spectrum with a Fermi-Dirac distribution. On ultrafast time scales, nonthermalized electrons have to be included [26,31], which leads to small corrections of the Fermi distribution for Gd. After normalization to f, the surface contributions $S^{\uparrow}$ and $S^{\downarrow}$ are clearly discernible [32]. Their energies with respect to E_F are shown in Fig. 3(a). For delays <2 ps, $E(S^{\uparrow})$ shifts towards E_F by only 45 meV. An analysis of such small changes is hindered for $E(S^{\downarrow})$ due to its larger linewidth and lower intensity, which leads to error bars larger than the shift of $E(S^{\uparrow})$. As seen from Fig. 3, we conclude that $\Delta_{\text{ex}} = E(S^{\downarrow}) + E(S^{\uparrow})$ remains constant within error bars at 600 ± 60 meV up to 1 ps [33]. This is remarkable because it demonstrates that Δ_{ex} is not determined by T_{el} [16].

Following Ref. [26] the transient electronic energy density $\varepsilon_{\text{el}}(t) = 2\int_0^{2\ \text{eV}} N(E, t)EdE$, where N is given by the PE spectra, is extracted and shown in Fig. 3(b). Compared to thermal equilibrium at -1 ps, ε_{el} has increased at 50 fs about a 100 times, which corresponds to a mean energy of $E_{\text{el}}/k_B = 1900$ K. The simultaneously observed drop in the $S^{\uparrow}$ population by 19% [inset of Fig. 3(b)] quantifies the intense optical excitation, as does the high nonequilibrium value of ε_{el}. ε_{el} decays by e-e and e-ph scattering and transport into the bulk [26,34]. The solid line shows a simulation of $\varepsilon_{\text{el}}(t)$ employing a two-temperature model [26]. ε_{el} decays within the first ps, which denotes the equilibration time of electron and lattice subsystems towards their common temperature of 220 K at 2 ps.

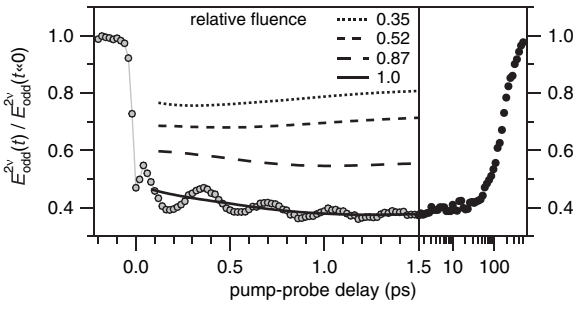

FIG. 1. Time-dependent odd second harmonic field representing the spin polarization of the Gd(0001) surface state. Lines depict the incoherent contribution for different relative pump fluences (maximum absorbed fluence ≈ 1 mJ/cm^2) after subtraction of the oscillatory part which is generated by a coherent phonon at the surface [25].

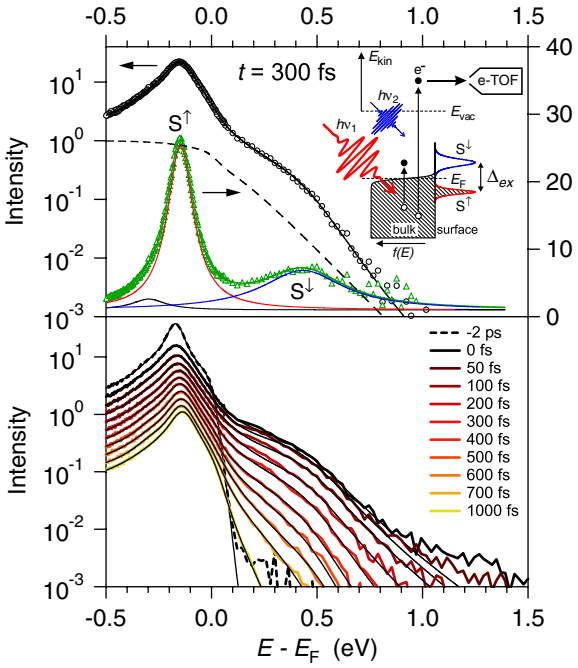

FIG. 2 (color online). Top: Normalized photoelectron spectrum at 300 fs (circles) with fit (solid line) and distribution function $f(E, t)$ (dashed line) on a logarithmic scale and divided by f (triangles) on a linear scale at right. The inset sketches the TRPE experiment. Bottom: Photoelectron spectra at different delays are displayed in color (fits in black) and are offset vertically.

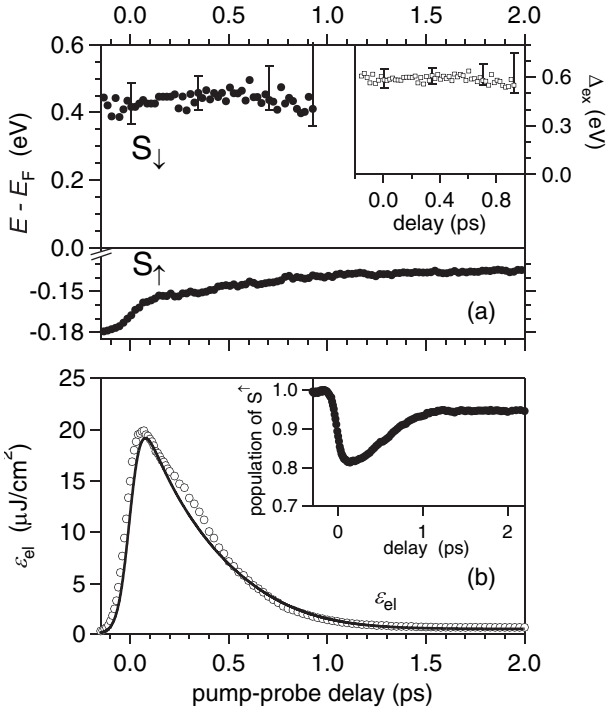

FIG. 3. (a) Energy positions of the occupied and unoccupied surface state components as a function of delay time with their energetic separation Δ_{ex} given in the inset. The error bars account for systematic deviations of the fitting procedure. (b) Transient energy density ε_{el} extracted from TRPE spectra (circles) representing the electron system. The solid line is a simulation following Ref. [26]. The inset depicts the population of $S^{\uparrow}$ normalized to the equilibrium value at 100 K.

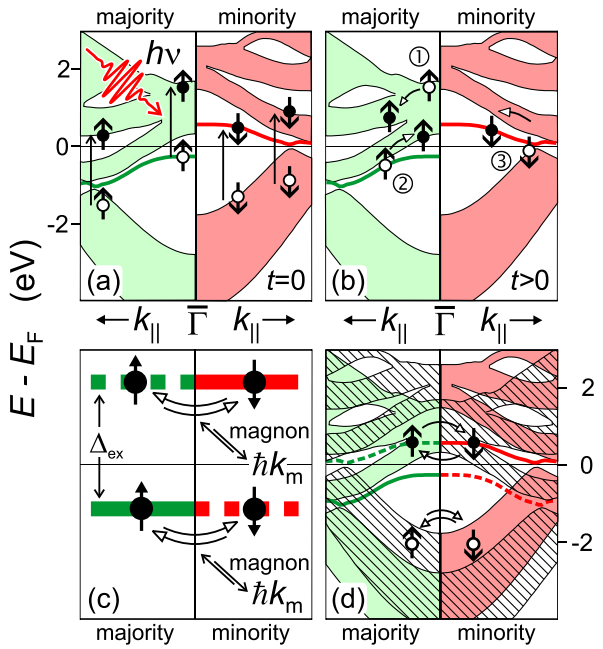

FIG. 4 (color online). Majority and minority electronic band structure of Gd(0001) based on Ref. [13]; areas represent bulk and lines surface states. The individual panels illustrate (a) optically excited electron-hole pairs, (b) exemplary *e-e* scattering events, (c),(d) electron-spin-flip scattering among spin-mixed states (dashed lines for the surface and hatched area for the bulk).

Summarizing the experimental results, we observe that after an intense excitation of the electronic system the spin polarization drops to half while the excess energy still resides in the electronic system and *e-e* scattering dominates. Since the exchange splitting remains constant, we can safely exclude a mechanism based on a reduced Δ_{ex} (Stoner behavior) and conclude that spin mixing prevails on the femtosecond time scale.

To develop a microscopic understanding of the ultrafast spin dynamics, we consider two contributions: (i) secondary electrons in combination with transport processes and (ii) spin-flip scattering of hot electrons among spin-mixed states. Figures 4(a) and 4(b) illustrate the optical excitation and secondary electron generation. The pump pulse excites $S^{\uparrow}$ electrons from the occupied surface state to unoccupied bulk states, minority electrons from bulk to unoccupied surface states, and transitions between bulk states. Transitions involving the surface state redistribute spin polarization from the surface to the bulk because majority electrons are excited into bulk states or minority electrons are excited to the surface state. This redistribution is a consequence of transport effects since the minority hole or majority electron, which is excited in the vicinity of the surface, propagates into the bulk. The decay of hot electrons generates secondary electrons, as observed in TRPE (Fig. 2). An individual event of *e-e* scattering [Fig. 4(b)] comprises electrons with identical spins; see, e.g., processes (1) and (2), or with opposite spins (Stoner excitations), c.f. (1) and (3). Both channels lower the spin polarization of the surface state on a time scale <100 fs. The above processes could explain the initial decrease in the spin polarization of the surface state within the laser pulse duration—but not of bulk states. However, the linewidth of the surface state components and the broad distribution function imply scattering rates above 0.1 fs^{-1} (Fig. 2 and Ref. [14]) and thus frequent scattering among surface and bulk states. Thus the surface spin polarization would be restored to its initial equilibrium value on the time scale of electron equilibration, which is clearly not observed (Fig. 1). Therefore further processes must be involved. Spin-orbit interaction has been suggested to transfer spin to orbital momentum [21,23]. It is very weak in Gd [35] and must be of minor importance here. Moreover, transitions among bulk bands and the d_{z^2} surface state do not change the orbital momentum since both are of *d* character [13].

We therefore turn to the second contribution, i.e., spin-flip scattering of electrons. As we have shown above, spin mixing prevails during the first picosecond after excitations. Thus a majority contribution at the minority state energy and a minority one for majority states is present [Figs. 4(c) and 4(d)] [2]. In this situation, an electron in the surface state can scatter quasielastically from the majority to the minority state by flipping its spin and reducing the

spin polarization [Fig. 4(c)]. The scattering probabilities are determined in part by the density of initial and final states. To conserve angular momentum, such spin-flip processes are balanced by the absorption or excitation of magnons which will also involve the $4f$ moments [12]. Consequently, the probability of this process is governed also by the strength of e-magnon interaction, which was shown for Gd to be comparable to e-ph interaction [36–39] and thus occurs on a femtosecond time scale. Since in thermal equilibrium spin mixing occurs for both bulk and surface states [8], we expect that e-magnon scattering in the ultrafast regime comprises both types of states as depicted in Fig. 4(d). e-magnon scattering represents a direct pathway to reduce the spin polarization through hot electrons, which store the excess energy during the collapse of the surface spin polarization. Consequently, we propose that spin-flip scattering of electrons is the dominant contribution. Furthermore, we speculate that e-magnon scattering is most effective for nonthermalized electrons, because the drop in $E^{2\nu}_{\mathrm{odd}}$ occurs within 100 fs.

In summary, we have demonstrated by this combined magneto-optical and photoemission study that the ultrafast dynamics of Δ_{ex} and M do not coincide for the Gd surface. Under nonequilibrium conditions, spin mixing dominates unambiguously over Stoner behavior. Electron-magnon interaction is proposed to facilitate electronic spin-flip scattering among surface and bulk states and to explain the observed loss in the spin polarization of the surface state within the first 100 fs. We expect that the present investigation furthers a microscopic understanding of femtosecond spin dynamics and questions the validity of the Stoner model under nonequilibrium conditions in general [21]. A theoretical description of the ultrafast loss of spin polarization thus requires the inclusion of spin-flip processes [40].

We are grateful to K. Starke and G. Kaindl for fruitful discussions and experimental support, and thank M. Weinelt for critically reading the manuscript. We acknowledge funding by the DFG through SPP 1133 and by the European Community which supported P. A. L. through Contract No. MEIF-CT-2003-501826.

*Electronic address: uwe.bovensiepen@physik.fu-berlin.de

[1] *Metallic Magnetism*, edited by H. Capellmann (Springer, Berlin, 1987).
[2] S. Rex, V. Eyert, and W. Nolting, J. Magn. Magn. Mater. **192**, 529 (1999).
[3] P. J. Brown, J. Deportes, D. Givord, and K. R. A. Ziebeck, J. Appl. Phys. **53**, 1973 (1982).
[4] W. von der Linden, M. Donath, and V. Dose, Phys. Rev. Lett. **71**, 899 (1993).
[5] T. Greber, T. J. Kreutz, and J. Osterwalder, Phys. Rev. Lett. **79**, 4465 (1997).
[6] A. Aharony, *Introduction to the Theory of Ferromagnetism* (Oxford University Press, New York, 2000), 2nd ed.
[7] W. Nolting *et al.*, Phys. Rev. B **40**, 5015 (1989).
[8] K. Maiti, M. C. Malagoli, A. Dallmeyer, and C. Carbone, Phys. Rev. Lett. **88**, 167205 (2002).
[9] D. Li, J. Pearson, S. D. Bader, D. N. McIlroy, C. Waldfried, and P. A. Dowben, Phys. Rev. B **51**, R13895 (1995).
[10] E. Weschke *et al.*, Phys. Rev. Lett. **77**, 3415 (1996).
[11] M. Bode *et al.*, Appl. Phys. A **66**, S121 (1998).
[12] A. V. Fedorov, T. Valla, F. Liu, P. D. Johnson, M. Weinert, and P. B. Allen, Phys. Rev. B **65**, 212409 (2002).
[13] P. Kurz, G. Bihlmayer, and S. Blügel, J. Phys. Condens. Matter **14**, 6353 (2002).
[14] A. Rehbein, D. Wegner, G. Kaindl, and A. Bauer, Phys. Rev. B **67**, 033403 (2003).
[15] E. Beaurepaire, J.-C. Merle, A. Daunois, and J.-Y. Bigot, Phys. Rev. Lett. **76**, 4250 (1996).
[16] J. Hohlfeld, E. Matthias, R. Knorren, and K. H. Bennemann, Phys. Rev. Lett. **78**, 4861 (1997).
[17] B. Koopmans, M. van Kampen, J. T. Kohlhepp, and W. J. M. de Jonge, Phys. Rev. Lett. **85**, 844 (2000).
[18] L. Guidoni, E. Beaurepaire, and J.-Y. Bigot, Phys. Rev. Lett. **89**, 017401 (2002).
[19] J.-Y. Bigot *et al.*, Phys. Rev. Lett. **93**, 077401 (2004).
[20] A. Scholl, L. Baumgarten, R. Jacquemin, and W. Eberhardt, Phys. Rev. Lett. **79**, 5146 (1997).
[21] H.-S. Rhie, H. A. Dürr, and W. Eberhardt, Phys. Rev. Lett. **90**, 247201 (2003).
[22] G. P. Zhang and W. Hübner, Phys. Rev. Lett. **85**, 3025 (2000).
[23] G. Zhang, W. Hübner, E. Beaurepaire, and J.-Y. Bigot, *Spin Dynamics in Confined Magnetic Structures I*, Topics in Applied Physics Vol. 83 (Springer, New York, 2002).
[24] B. Koopmans, *Spin Dynamics in Confined Magnetic Structures II*, Topics in Applied Physics Vol. 87 (Springer, New York, 2003).
[25] A. Melnikov *et al.*, Phys. Rev. Lett. **91**, 227403 (2003).
[26] M. Lisowski *et al.*, Appl. Phys. A **78**, 165 (2004).
[27] R.-P. Pan, H. D. Wei, and Y. R. Shen, Phys. Rev. B **39**, 1229 (1989).
[28] A. Melnikov *et al.*, Appl. Phys. B **74**, 723 (2002).
[29] A. Vaterlaus, T. Beutler, and F. Meier, Phys. Rev. Lett. **67**, 3314 (1991).
[30] A weak peak at -0.3 eV, which has been attributed in Ref. [14] to tip induced effects, is included as well.
[31] W. S. Fann, R. Storz, H. W. K. Tom, and J. Bokor, Phys. Rev. B **46**, 13 592 (1992).
[32] In the case of Ni [21] this was not possible at delays <1 ps.
[33] The constant Δ_{ex} is also found, albeit 25 meV larger, if $f(E, t)$ is a simple Fermi-Dirac distribution. Corrections for nonthermalized electrons improve the fit stability.
[34] J. Hohlfeld *et al.*, Chem. Phys. **251**, 237 (2000).
[35] M. Colarieti-Tosti *et al.*, Phys. Rev. Lett. **91**, 157201 (2003).
[36] P. Fulde and J. Jensen, Phys. Rev. B **27**, 4085 (1983).
[37] S. A. Sondhelm and R. C. Young, J. Phys. F **15**, L261 (1985).
[38] H. L. Skriver and I. Mertig, Phys. Rev. B **41**, 6553 (1990).
[39] E. Hatta *et al.*, J. Phys. Soc. Jpn. **70**, 1865 (2001).
[40] V. P. Zhukov, E. V. Chulkov, and P. M. Echenique, Phys. Rev. Lett. **93**, 096401 (2004).